



www.sciencemag.org/cgi/content/full/335/6071/970/DC1

Supporting Online Material for

Control of Nonapoptotic Developmental Cell Death in *Caenorhabditis elegans* by a Polyglutamine-Repeat Protein

Elyse S. Blum, Mary C. Abraham, Satoshi Yoshimura, Yun Lu, Shai Shaham*

*To whom correspondence should be addressed. E-mail shaham@rockefeller.edu

Published 24 February 2012, *Science* **335**, 970 (2012)

DOI: 10.1126/science.1215156

This PDF file includes:

Materials and Methods

Figs. S1 to S13

Tables S1 and S2

References (25–65)

Materials and Methods*Strains*

C. elegans strains were cultured using standard methods (25, 26), and were maintained at 20°C. Wild-type animals were Bristol variety N2. The following alleles were crossed with *qIs56* V (27), an integrated GFP transgene to mark the linker cell, and *him-8(e1489)* IV or *him-5(e1490)* V (28) to increase the incidence of males:
 LGI: *dlk-1(tm4024)* (Japanese National BioResource Project), *mtk-1(ok1382)* (*C. elegans* Gene Knockout Consortium), *tol-1(nr2033)* (29)
 LGII: *lin-29(n333)* (30), *rrf-3(pk1426)* (14), *nsy-1(ky397, ky542)* (31)
 LGIII: *pqn-41(ns294)*, *tir-1(qd4)* (32), *mpk-1(ku1)* (33)
 LGIV: *pmk-1(km25)* (34), *pmk-3(ok169)* (35, 36), *jnk-1(gk7)* (37), *kgb-1(km21)* (34), *kgb-2(gk361)* (*C. elegans* Gene Knockout Consortium)
 LGV: *rde-1(ne219)* (16)
 LGX: *sek-1(ag1; km4)* (38, 39), *jkk-1(km2)* (40), *mek-1(ks54)* (41), *mkk-4(ju91)* (36)

Transgenic strains:

Transgene	Constructs	Reference
<i>nsEx3131</i>	pMA5 (<i>pqn-41</i> (2.5kb) pro::GFP) + <i>unc-119</i> (+)	This work
<i>nsEx1696-1698</i>	pMA5 (<i>pqn-41</i> (2.5kb) pro::GFP) (20ng/ul) + pRF4 (30ng/ul) + pSL1180 (50ng/ul)	This work
<i>nsEx2590</i>	pEB18 (<i>pqn-41</i> (13kb) pro::GFP) + <i>unc-119</i> (+)	This work
<i>nsEx903</i>	3.5kb <i>lin-29A</i> pro::GFP + pRF4	(8)
<i>nsEx2584</i>	pEB17 (<i>sek-1</i> pro::GFP) + <i>unc-119</i> (+)	This work
<i>qIs56</i>	<i>lag-2</i> pro::GFP	(27)
<i>nsEx3081</i>	<i>mig-24</i> pro:: <i>rde-1</i> cDNA::SL2::mCherry + <i>lag-2</i> p::mCherry	Gift from M. Kinet
<i>nsEx3132</i> , <i>nsEx3168</i> , <i>nsEx3204</i>	pEB21 (<i>mig-24</i> pro:: <i>pqn-41</i> A cDNA) + <i>lag-2</i> pro::GFP	This work
<i>nsEx3402</i> , <i>nsEx3403</i> , <i>nsEx3381</i> , <i>nsEx3404</i>	pEB38 (<i>mig-24</i> pro:: <i>pqn-41</i> B cDNA)+ <i>lag-2</i> pro::GFP	This work
<i>nsEx3161</i> , <i>nsEx3166</i> , <i>nsEx2916</i> , <i>nsEx2917</i> , <i>nsEx2358</i>	pEB26 (<i>mig-24</i> pro:: <i>pqn-41</i> C cDNA)+ <i>lag-2</i> pro::YFP	This work
<i>nsEx2867</i> , <i>nsEx2868</i>	<i>lin-48</i> pro:: <i>sek-1</i> cDNA::SL2::mCherry + pRF4	This work
<i>nsEx3191</i>	pEB16 (<i>mig24</i> pro:: <i>sek-1</i> cDNA:: <i>sek-1</i> 3' UTR) (25ng/ul) + pRF4 (25ng/ul) + pSL1180 (50ng/ul)	This work
<i>nsEx2867</i> , <i>nsEx2868</i>	<i>mig-24</i> pro:: <i>sek-1</i> cDNA::SL2::mCherry + pSL1180	This work
<i>nsEx3191</i>	pEB22 (<i>mig-24</i> pro:: <i>pqn-41</i> A cDNA::GFP)+ <i>unc-119</i> (+)	This work
<i>nsEx3192</i>	pEB24 (<i>mig-24</i> pro:: <i>pqn-41</i> B cDNA::GFP)+ <i>unc-119</i> (+)	This work
<i>nsEx3134 - 3137</i>	pEB28 (<i>mig-24</i> pro:: <i>pqn-41</i> C cDNA::GFP) + <i>unc-119</i> (+)	This work

<i>nsEx3394</i> , <i>nsEx3378</i> , <i>nsEx3395</i>	pEB27 (<i>mig-24pro::pqn-41</i> C exons 4 and 5) + <i>lag-2pro::YFP</i>	This work
<i>nsEx3379</i>	pEB32 (<i>mig-24pro::pqn-41</i> C cDNA)+ <i>lag-2pro::YFP</i>	This work
<i>nsEx3380</i> , <i>nsEx3396</i>	pEB33 (<i>mig-24pro::pqn-41</i> B N-terminus)+ <i>lag-2pro::YFP</i>	This work
<i>nsEx3420</i>	pEB34 (<i>mig-24pro::pqn-41</i> C Δ CC1-2)+ <i>lag-2pro::YFP</i>	This work
<i>nsEx3397</i> , <i>nsEx3398</i> , <i>nsEx3399</i>	pEB35 (<i>mig-24pro::pqn-41</i> C Δ CC3-4)+ <i>lag-2pro::YFP</i>	This work
<i>nsEx3400</i> , <i>nsEx3401</i>	pEB36 (<i>mig-24pro::pqn-41</i> C Δ CC5-6)+ <i>lag-2pro::YFP</i>	This work
<i>nsEx3384</i> <i>nsEx3385</i> <i>nsEx3386</i>	pEB37 (<i>cdh-3pro::pqn-41</i> C) + <i>lag-2pro::YFP</i>	This work
<i>nsEx3405</i> , <i>nsEx3406</i>	pEB39 (<i>mig-24pro::pqn-41</i> C Proline sub.)+ <i>lag-2pro::YFP</i>	This work
<i>nsEx3407</i> , <i>nsEx3408</i>	pEB40 (<i>mig-24pro::pqn-41</i> C Δ M1-A27)+ <i>lag-2pro::YFP</i>	This work
<i>nsEx3409</i> , <i>nsEx3410</i>	pEB41 (<i>mig-24pro::pqn-41</i> C Δ A80-V98)+ <i>lag-2pro::YFP</i>	This work
<i>nsEx3411</i>	pEB42 (<i>mig-24pro::pqn-41</i> C Δ Q417-R427)+ <i>lag-2pro::YFP</i>	This work
<i>nsEx3412</i> , <i>nsEx3413</i> , <i>nsEx3414</i>	pEB43 (<i>mig-24pro::pqn-41</i> B Δ N-terminal CC domains 1)+ <i>lag-2pro::YFP</i>	This work
<i>nsEx3415</i> , <i>nsEx3416</i>	pEB44 (<i>mig-24pro::pqn-41</i> B Δ C-terminal CC domains 2)+ <i>lag-2pro::YFP</i>	This work

RNA interference assay

RNAi was performed by feeding (42-44). The OS2570 (*rrf-3(pk1426)* II; *him-8(e1489)* IV; *qIs56* V) strain was used for the screen. Bleached embryos from OS2570 gravid hermaphrodites were left in M9 overnight to synchronize at the L1 stage. 250 L1s, of which ~30% were male, were added to each RNAi plate. Animals were grown at 20-22°C, and scored 48 hours later, when they were approximately 2-4 h adults, using a fluorescent dissecting scope (Leica). We used published clones from the Ahringer feeding library (45, 46). Of the 16,757 library clones, only 16,208 clones were screened as 549 failed to grow. In addition, 1,924 non-overlapping clones from the ORFeome-based RNAi library (47) were scored. Combined, the libraries represent 89% of the 20,416 *C. elegans* protein coding sequences based on Wormbase curated version WS221. For the genome-wide screen, 12-well RNAi plates were made by adding Isopropyl-beta-D-1-thiogalactopyranoside (IPTG; Sigma-Aldrich; 1 mM final) and Carbenicillin (Novagen; 25 ug/mL final) to standard NGM agar (26), and were used within 10 days of pouring. Glycerol stocks of the RNAi clones were thawed and inoculated into 96 well plates containing 225 ul LB with Ampicillin (50 ug/mL) using the PerkinElmer Life Sciences MiniTrak V liquid handling robot. Cultures were grown overnight at 37°C without shaking. The 12-well RNAi plates were then seeded with 175 ul of the overnight

culture using a Perkin Elmer MultiProbe II HT EX liquid handling machine. At least two hours after seeding, 250 synchronized L1s were added to each well. The empty RNAi clone vector, L4440, was used as a negative control along with a GFP RNAi clone as a positive control.

Generating *pqn-41(ns294)*

pqn-41(ns294) deletion mutant was isolated using published methods (48, 49). The following primer pairs (5' to 3') were used for screening *pqn-41*: poison primer GCAATCACAGGAGAAGAAGCTTCCG; inner primers, CACATAAATCACCCCTTTTCTATCCGCC and CGATTTCCCTCGTCATTTTCTACCGC; outer primers, AACACCGCAGAGCCTTACGAC and GTAAGGCGCTTCGTGGTTGC. The strain was backcrossed to N2 five times after isolation. The deletion spans a region from 145 bp upstream of exon 18 to 192 nucleotides downstream of the exon 18 start site.

Germline transformation

Germline transformation was carried out as described (50). For *pqn-41* rescue studies all plasmids were injected into *pqn-41(ns294)* III; *him-8(e1489)* IV hermaphrodites with *lag-2pro::YFP* as a transformation marker (gift from Mihoko Kato and Paul Sternberg, (51)). For GFP expression studies, all plasmids were injected into *unc-119(ed3)* III; *him-8(e1489)* IV hermaphrodites with *unc-119(+)* (52) as a transformation marker, unless otherwise noted. Several transgenic lines containing the *pqn-41*(2.5 kb) *pro::GFP* construct were generated for this study having the genotypes: *unc-119(ed3) him-8(e1489); nsEx3131, him-5(e1490); nsEx2364 and him-5(e1467); nsEx1696-1698*. All plasmids were injected at 50 ng/ul unless otherwise noted. pSL1180 is an empty cloning vector used to increase the DNA concentration of injection mixtures.

Plasmid Construction

All primers sequences written 5' to 3'

Construct	Description	Notes
pRF4	<i>rol-6(su1006)</i>	(50)
pMA5	<i>pqn-41</i> (2.5kb) <i>pro::GFP</i>	N2 genomic sequence was amplified using primers: 5'-CTGACTCTAGAGCGGGACAATGC and 5'-ACAGTACCGGTAGCATTCCACTCCAG and ligated into pPD95.75 (Andrew Fire) as an XbaI/AgeI fragment.
pEB16	<i>mig-24pro::sek-1</i> cDNA:: <i>sek-1</i> 3' UTR	<i>sek-1</i> cDNA:: <i>sek-1</i> 3'UTR was amplified from <i>odr-3p::sek-1</i> cDNA construct, gift from Kunihiro Matsumoto (53), using 5'-gtctctctagagGTACCCatcatggag and 5'-ttttttACtAGtaaaaaaaatcttactcgagc. This KpnI/SpeI fragment was ligated into pPD95.79 (Andrew Fire) containing <i>mig-24</i> promoter (gift from Kiyoji Nishiwaki) between BamHI/KpnI.
pEB17	4.6 kb <i>sek-1pro::GFP</i>	4.6 kb of N2 genomic DNA was amplified using primers 5'-ctaagagcatgctagaaacttatgagtgttctgtg and

		5'- gatttttcttaAcCGGtcgctccatgatgtaag. The amplicon was ligated into pPD95.75 (Andrew Fire) as an SphI/AgeI fragment.
pEB18	<i>pqn-41</i> (13kb) pro::GFP	N2 genomic sequence was amplified in sections starting with the left most primer 5'- ggcttctggtGCATGCggcttaccagagg-3' containing an SphI site. The right most primer 5'- gataaaatcgaC CGGtcgctccattc abolishes the stop codon and contains an AgeI site. The SphI/AgeI fragment was ligated into pPD95,75.
pEB21	<i>mig-24</i> pro:: <i>pqn-41A</i> cDNA	<i>pqn-41</i> cDNA was amplified in fragments from cDNA libraries generated from N2 animals. Endogenous restriction sites were used to ligate amplicons. The <i>mig-24</i> pro was cloned as an NotI/FseI fragment into the pSM vector (Cori Bargmann).
pEB22	<i>mig-24</i> pro:: <i>pqn-41A</i> cDNA::GFP	pEB13 (<i>pqn-41</i> (2.5kb) pro::F53A3.4cDNA::GFP in pPD95.75, Addgene) was digested with BglII/ApaI to generate a fragment containing the last two <i>pqn-41</i> exons with the stop codon abolished in frame with GFP – <i>unc-54</i> 3'UTR. This was then ligated into pEB21.
pEB24	<i>mig-24</i> pro:: <i>pqn-41B</i> cDNA::GFP	pEB13 (<i>pqn-41</i> (2.5kb) pro::F53A3.4cDNA::GFP in pPD95.75, Addgene) was digested with BglII/ApaI to generate a fragment containing the last two <i>pqn-41</i> exons with the stop codon abolished in frame with GFP – <i>unc-54</i> 3'UTR. This was then ligated into pEB23.
pEB27	<i>mig-24</i> pro:: <i>pqn-41C</i> exons 4 and 5	The cDNA sequence was amplified as a KpnI/BglII fragment from pEB26 using primers ccagCTCCAACcggTAAATGGAACG and CAGACGAATAAGATCTTGGCCATTTCGGTC. The amplicon was then ligated back into KpnI/BglII digested pEB26.
pEB28	<i>mig-24</i> pro:: <i>pqn-41 C</i> cDNA::GFP	pEB13 (<i>pqn-41</i> (2.5kb) pro::F53A3.4cDNA::GFP in pPD95.75, Addgene) was digested with BglII/ApaI to generate a fragment containing the last two <i>pqn-41</i> exons with the stop codon abolished in frame with GFP – <i>unc-54</i> 3'UTR. This was then ligated into pEB26.
pEB30	<i>lag-2p</i> ::mCherry	An AgeI/SpeI fragment containing mCherry:: <i>unc-54</i> 3'UTR from the <i>mig-24p</i> ::mCherry plasmid was ligated into AgeI/SpeI digested <i>lag-2p</i> ::YFP plasmid (gift from Mihoko Kato and Paul Sternberg, (51)).
pEB32	<i>mig-24</i> pro:: <i>pqn-41C</i>	The cDNA C sequence was amplified as a

	cDNA	KpnI/BglII fragment from pEB23 (<i>mig-24</i> pro:: <i>pqn-41</i> B cDNA). This was then ligated to KpnI/BglII digested pEB19 (<i>mig-24</i> pro::F53A3.4 cDNA, pPD95.75, Addgene) between the <i>mig-24</i> promoter and the second to last exon of <i>pqn-41</i> . This created pEB26, which contains a Q66H mutation in the cDNA. pEB32 contains the corrected WT cDNA sequence, and behaves the same as pEB26.
pEB33	<i>mig-24</i> pro:: <i>pqn-41</i> BΔpolyQ	The cDNA sequence was amplified as a NsiI/SacII fragment from pEB23 using primers gtcGCTGGAGTGGAAAtcaTGTA AAAATTG and cggaaattCCgCgGattgtcACGATTGTTGATGTTGC GAC. The amplicon was ligated into <i>mig-24</i> p::1-4495 cDNA in pSM (Derived from pPD95.75, Addgene) using NsiI/SacII.
pEB34	<i>mig-24</i> pro:: <i>pqn-41</i> CΔ 33-139aa	The deletion in PQN-41C coiled-coil domains 1 and 2 was generated using PCR splicing (http://www.methods.info/Methods/Mutagenesis/PCR_splicing.html). The amplicon was ligated into pEB26 as a KpnI/EcoRI fragment.
pEB35	<i>mig-24</i> pro:: <i>pqn-41</i> CΔ 151-277aa	The deletion in PQN-41C coiled-coil domains 1 and 2 was generated using PCR splicing (http://www.methods.info/Methods/Mutagenesis/PCR_splicing.html). The amplicon was ligated into pEB26 as a KpnI/EcoRI fragment.
pEB36	<i>mig-24</i> pro:: <i>pqn-41</i> CΔ 286-397aa	The deletion in PQN-41C coiled-coil domains 1 and 2 was generated using PCR splicing (http://www.methods.info/Methods/Mutagenesis/PCR_splicing.html). The amplicon was ligated into pEB26 as a KpnI/EcoRI fragment.
pEB37	<i>cdh-3</i> pro:: <i>pqn-41</i> C	The <i>cdh-3</i> promoter was amplified from N2 genomic DNA as a BamHI/KpnI fragment using primers gaagcttttggtagGgAtCctgtaattttg and gaacaacaacggTACcgagaccttaattgttc. The amplicon was ligated into pEB32.
pEB39	<i>mig-24</i> pro:: <i>pqn-41</i> C coiled coil defective	Two proline substitutions were introduced into the middle of PQN-41 C coiled coil domains 2, 4, and 6 using a modified PCR splicing strategy. Using pEB32 as the template, four PCR reactions were performed using the following primer sets: tggcgGTACCCATGGCGGCTGCAATAAATG and

		<p>CTGTTCTCTTTGCgGTTGTTGTgGTTGTTGTTGCAG; CTGCAACAACAACcACAACAACcGCAAAGAGAACAG and GTGCCTGCGCCTGTGgCTGAGCAgGTGCCTGCTGTACCTG; CAGGTACAGCAGGCACcTGCTCAGcCACAGGCGCAGGCAC and GAGCTTGAGCCTGGGgGGCTGCTGgGGCGGCCTGTTGCTG;</p> <p>CAGCAACAGGCCGCCcCAGCAGCCcCCCAGGCTCAAGCTC and CTCAGTTGGAATTCATCGTCCATTC. The individual PCR reactions were gel extracted and used as the template for a final round of PCR using the first and last primers listed above. This produced an amplicon flanked by KpnI/EcoRI sites that was then ligated back into pEB32.</p>
pEB40	<i>mig-24</i> pro:: <i>pqn-41C</i> ΔM1-A27aa	The deletion in PQN-41C conserved domain was generated using PCR splicing (http://www.methods.info/Methods/Mutagenesis/PCR_splicing.html). The final amplicon was ligated into pEB32 as a KpnI/BglIII fragment.
pEB41	<i>mig-24</i> pro:: <i>pqn-41C</i> ΔA80-V98aa	The deletion in PQN-41C conserved domain was generated using PCR splicing (http://www.methods.info/Methods/Mutagenesis/PCR_splicing.html). The final amplicon was ligated into pEB32 as a KpnI/BglIII fragment.
pEB42	<i>mig-24</i> pro:: <i>pqn-41C</i> ΔQ417-R427aa	The deletion in PQN-41C conserved domain was generated using PCR splicing (http://www.methods.info/Methods/Mutagenesis/PCR_splicing.html). The final amplicon was ligated into pEB32 as a BglIII/EcoRI fragment.
pEB43	<i>mig-24</i> pro:: <i>pqn-41B</i> Δ263-440aa	The deletion in PQN-41B N terminal coiled coil region 1 was generated using PCR splicing (http://www.methods.info/Methods/Mutagenesis/PCR_splicing.html). The final amplicon was ligated into pEB38 as an EcoRV/NsiI fragment.
pEB44	<i>mig-24</i> pro:: <i>pqn-41B</i> Δ683-892aa	The deletion in PQN-41B N terminal coiled coil region 2 was generated using PCR splicing (http://www.methods.info/Methods/Mutagenesis/PCR_splicing.html). The final amplicon was ligated into pEB38 as an EcoRV/NsiI fragment.
	<i>lin-48</i> pro:: <i>sek-1</i> cDNA::SL2:mCherry	<i>lin-48</i> promoter was amplified from N2 genomic DNA using primers 5-

		gaaaatatggcCGgCCttttgatgatg and 5'-caatcagcgCTagccatacccgatgaatc, and inserted into pSM-SL2-mCherry vector (Cori Bargmann) as a FseI/NheI fragment. <i>sek-1</i> cDNA was amplified from pEB16 using primers 5'-aatggcgGTcgacatcATGGAGCGAAAAG and 5'-ATTCGGCggtaCCGATGCtcaTCGTCGCCAAAC, and ligated into vector as a Sall/KpnI fragment.
	<i>mig-24</i> pro:: <i>sek-1</i> cDNA::SL2:mCherry	The <i>mig-24</i> promoter was amplified from <i>mig-24</i> p::mCherry construct using primers 5'-GTCTACTCTAGAGGccggectatcagttatc and 5'-ctACCGGgctagccatttaataaaattgtgtaag. The FseI/NheI fragment was then ligated into digested <i>lin-48</i> pro:: <i>sek-1</i> cDNA::SL2-mCherry construct.
	<i>mig-24</i> pro:: <i>rde-1</i> cDNA::SL2::mCherry	The <i>mig-24</i> promoter was ligated into pSM-SL2-mCherry vector as a BamHI/KpnI fragment. The <i>rde-1</i> cDNA was amplified in fragments from cDNA isolated from N2 animals. The full cDNA was ligated as a KpnI/KpnI fragment. (gift from Maxime Kinet).

lin-29(n333) sequencing

Genomic DNA was purified from *lin-29(n333); qIs56 him-5(e1490)* animals. Primer sets were designed within intronic sequences to amplify each exon including splice donor/acceptor sites. In *lin-29(n333)* mutants, the splice acceptor of exon 5 was found to have a G to A mutation at the conserved splice acceptor site.

pqn-41 transcripts

Structures of the *pqn-41A* and *B* transcripts were suggested by Wormbase (www.wormbase.org) predictions and verified using RT PCR. *pqn-41C* structure was suggested by RNAseq experiments (54, 55) and confirmed by PCR. All three transcripts are trans-spliced to the SL1 spliced leader.

pqn-41C ectopic expression

pqn-41C was expressed in the distal tip cell using the *mig-24* promoter (pEB32). Expression in the anchor cell was induced using a *cdh-3* promoter fragment (56) in plasmid pEB37. In both cases defects in the presence of cells as well as egg-laying defects were examined and none were found.

Cell Survival Assay

Late L4-stage males were defined by having maximal tail retraction completely to the base of the tail taper. Two hours from this stage was defined as a zero-hour adult male. Linker cell death was scored at various time points after this stage, and was recorded if both fluorescence and DIC microscopy revealed either the complete absence of a GFP-marked linker cell, or a linker cell with a corpse morphology characterized by

cell rounding, cytoplasmic volume reduction, nuclear envelope breakdown, or large-scale blebbing. Extra cells in the anterior pharynx were counted by DIC microscopy (57).

Scoring pqn-41 expression

0-2 hour adult *lin-29* or *sek-1* mutant males containing the *nsEx3131* transgene were scored for the presence of a GFP expressing linker cell in the cloacal region or along the linker cell migration path. The fraction of animals expressing GFP was then divided by the fraction of animals with surviving linker cells displayed in Fig. 4B.

Light microscopy

Linker cell death scoring and GFP expression patterns were analyzed by conventional fluorescence microscopy using an Axioplan II compound microscope (Zeiss) equipped with an AxioCam CCD camera (Zeiss). Images were acquired and analyzed using AxioVision (Zeiss). Alternatively, images were acquired using DeltaVision Image Restoration Microscope (Applied Precision) equipped with a Photometrics CoolSnap CCD camera (Roper Scientific). Acquisition, deconvolution, and analysis of DeltaVision images were performed with Softworx (Applied Precision).

Electron Microscopy

Two to three hour adult males of the genotype *pqn-41(ns294)* III; *qIs56 him-5(e1490)* V with surviving linker cells were first imaged using an Axioplan II compound microscope (Zeiss) to record the position of the linker cell. Animals were then fixed, stained, embedded in resin, and serially sectioned using standard methods (58). Images were taken with a FEI Technai G2 Spirit BioTwin transmission electron microscope with a Gatan 4K X 4K digital camera.

Statistical methods

All comparisons employed chi-squared statistics.

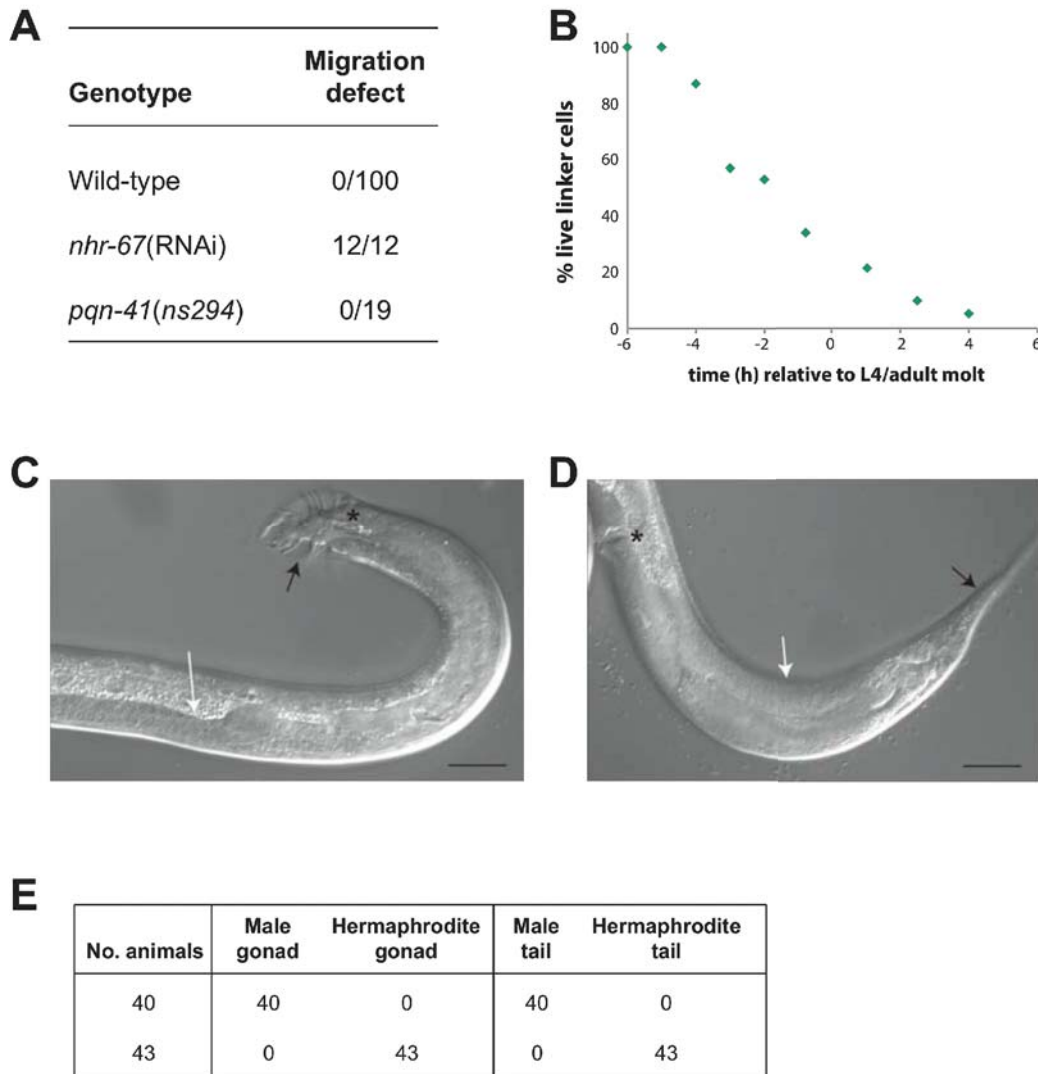


fig. S1. *pqn-41* is not required for linker cell migration or *C. elegans* sex determination. (A) Males of the indicated genotypes were assessed for linker cell migration defects. Number of migration defective cells/total number of surviving linker cells (*nhr-67*, *pqn-41*) or total animals observed (wild type). *nhr-67*(RNAi) is a positive control (51). (B) Chromosomally XX animals of the genotype *tra-2(ar221ts)*; *xol-1(y9)*; *mig-24* promoter::GFP (integrated transgene) were grown at 25° to promote male development (59), and the proportion of animals with visible linker cells were examined at the indicated time points (n>50 for each time point). The observed kinetics match those previously described for XO males (8), indicating that the linker cell dies normally in these masculinized XX hermaphrodites despite other morphological features, such as tail structure, that do not fully transform to the male pattern. (C, D) Male and hermaphrodite *pqn-41*(*ns294*) animals, respectively. Note full sexual differentiation of both tail soma (black arrow), gonad (white arrow), and mating structures (asterisks). Scale bar, 50 microns. (E) Table showing a perfect correlation between gonadal and somatic sex in *pqn-41*(*ns294*) mutants, indicative of no defects in sex determination.

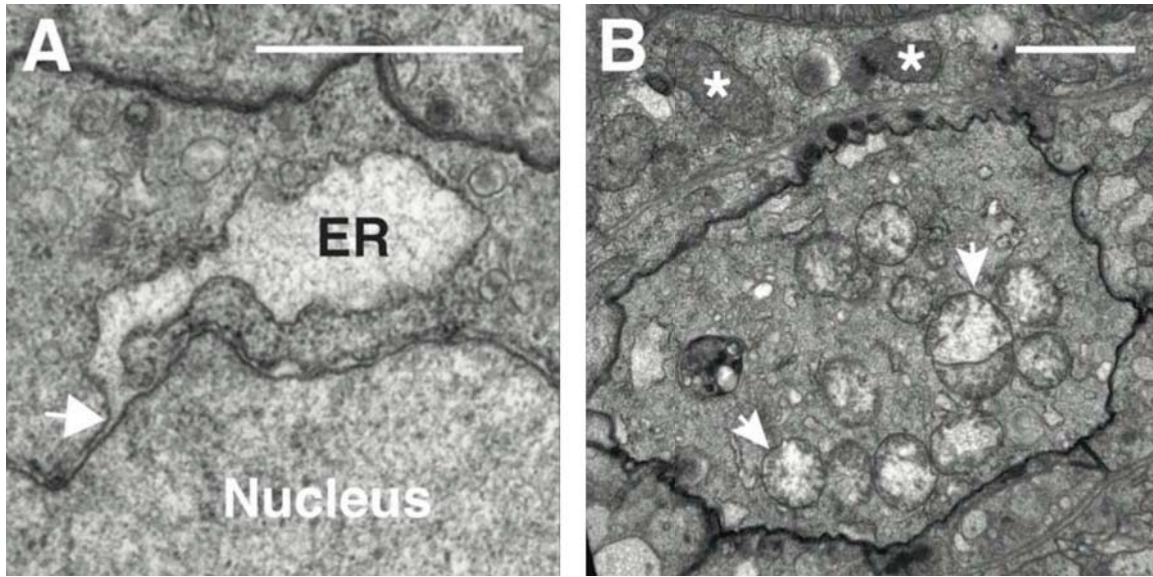


fig. S2. EM of surviving linker cell in Fig. 1D. **(A)** Enlargement of dashed box in Fig. 1D. ER, endoplasmic reticulum. Arrow points to where the outer nuclear membrane is abnormally expanded. **(B)** Swollen and lightly staining mitochondria (arrows) in linker cell shown in Fig. 1D. Asterisks, normal mitochondria in neighboring cell. Scale bars in **(A, B)**, 2 μm .

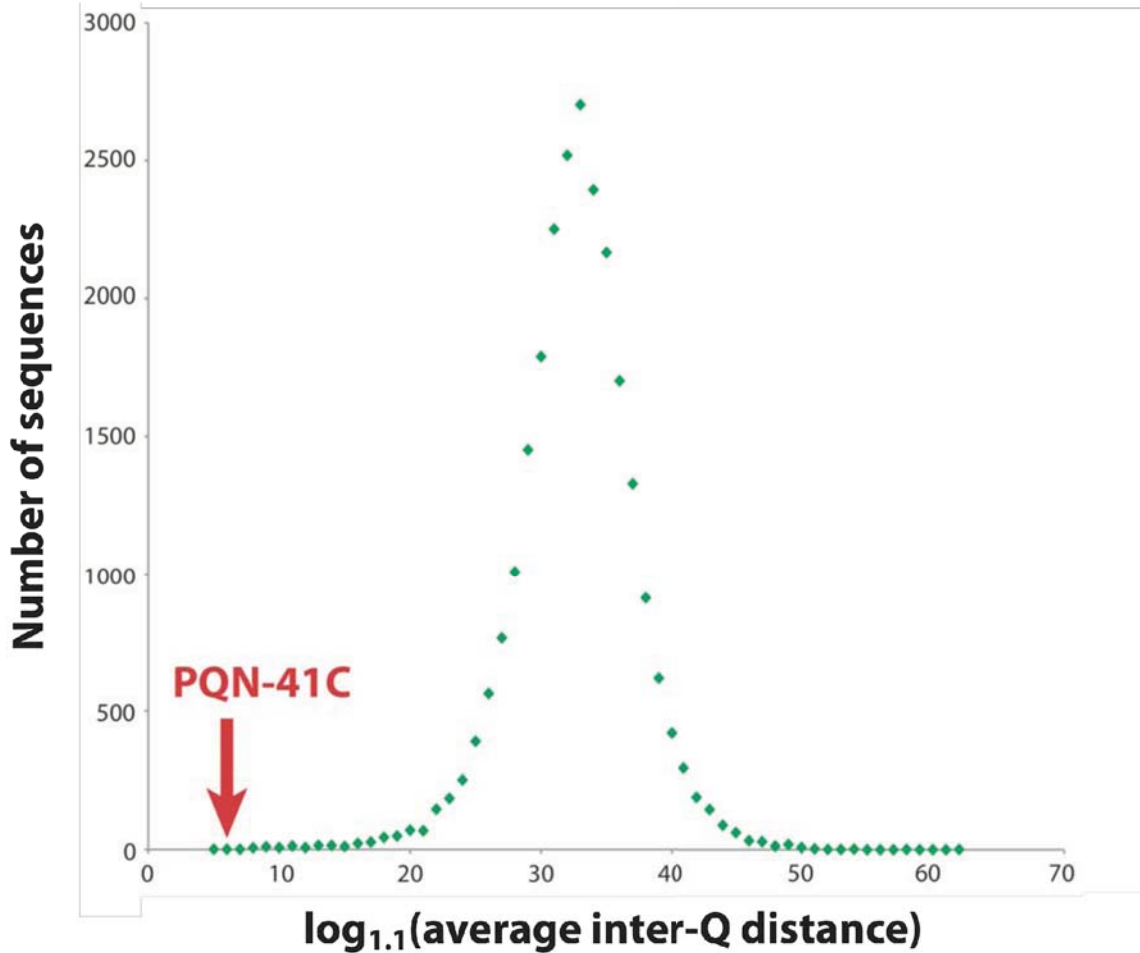


fig. S4. The average inter-glutamine distance in PQN-41C is the second smallest in the predicted *C. elegans* proteome. Plot of the number of predicted protein sequences in the *C. elegans* genome containing a given average inter-Q distance. The number of proteins with an average inter-Q distance between two consecutive powers of 1.1 was determined using a custom perl script, and plotted. The log base of 1.1 was used to give the tightest fit to the log-normal distribution.

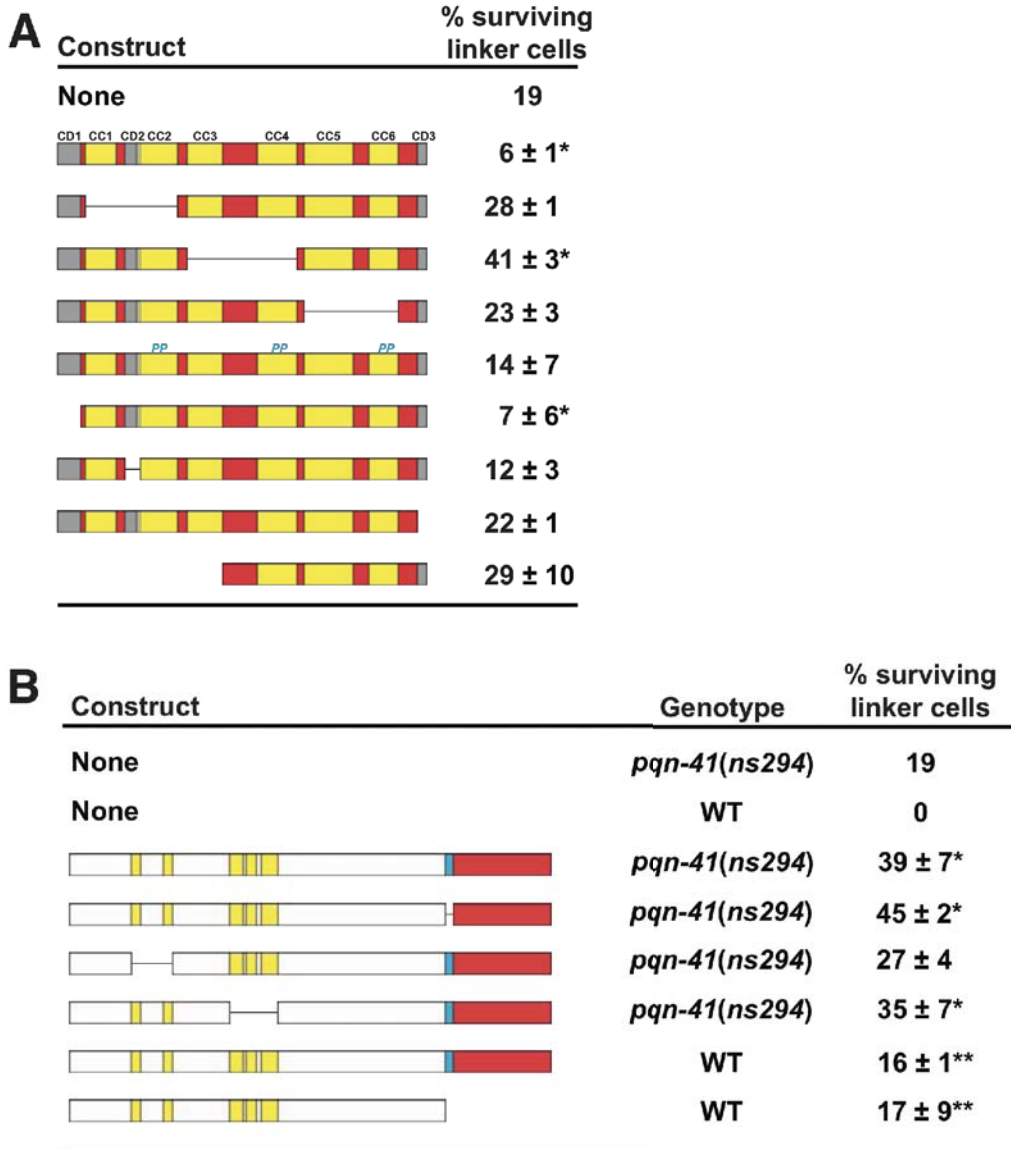


fig. S6. Structure/function dissection of PQN-41. (A) Table showing the effects of expressing wild-type and mutant versions of PQN-41C on linker cell survival in *pqn-41(ns294)* mutants. *, significantly different from *pqn-41(ns294)*, $p < 0.01$. Numbers are averages of the means \pm SD of two or more independent lines, except for CC1/2 deletion, where only one line was obtained, and error is SEM. $n > 50$ for each line. Yellow, predicted coiled-coil. Gray, regions conserved in nematodes. Red, linker domains between coiled coils. Coil-breaking Proline mutations are indicated in blue. CC, coiled coil. CD, conserved domain. (B) Table showing the effects of expressing wild-type and mutant versions of *pqn-41A* and *B* on linker cell survival in wild-type or *pqn-41(ns294)* animals. Color codes are as in Fig. 2C. *, significantly different from *pqn-41(ns294)*, $p < 0.01$. **, significantly different from wild type, $p < 0.01$. Numbers are averages of the means \pm SD of two or more independent lines, except for *pqn-41B* expression in wild type where only one line was scored and error is SEM. $n > 50$ for each line.

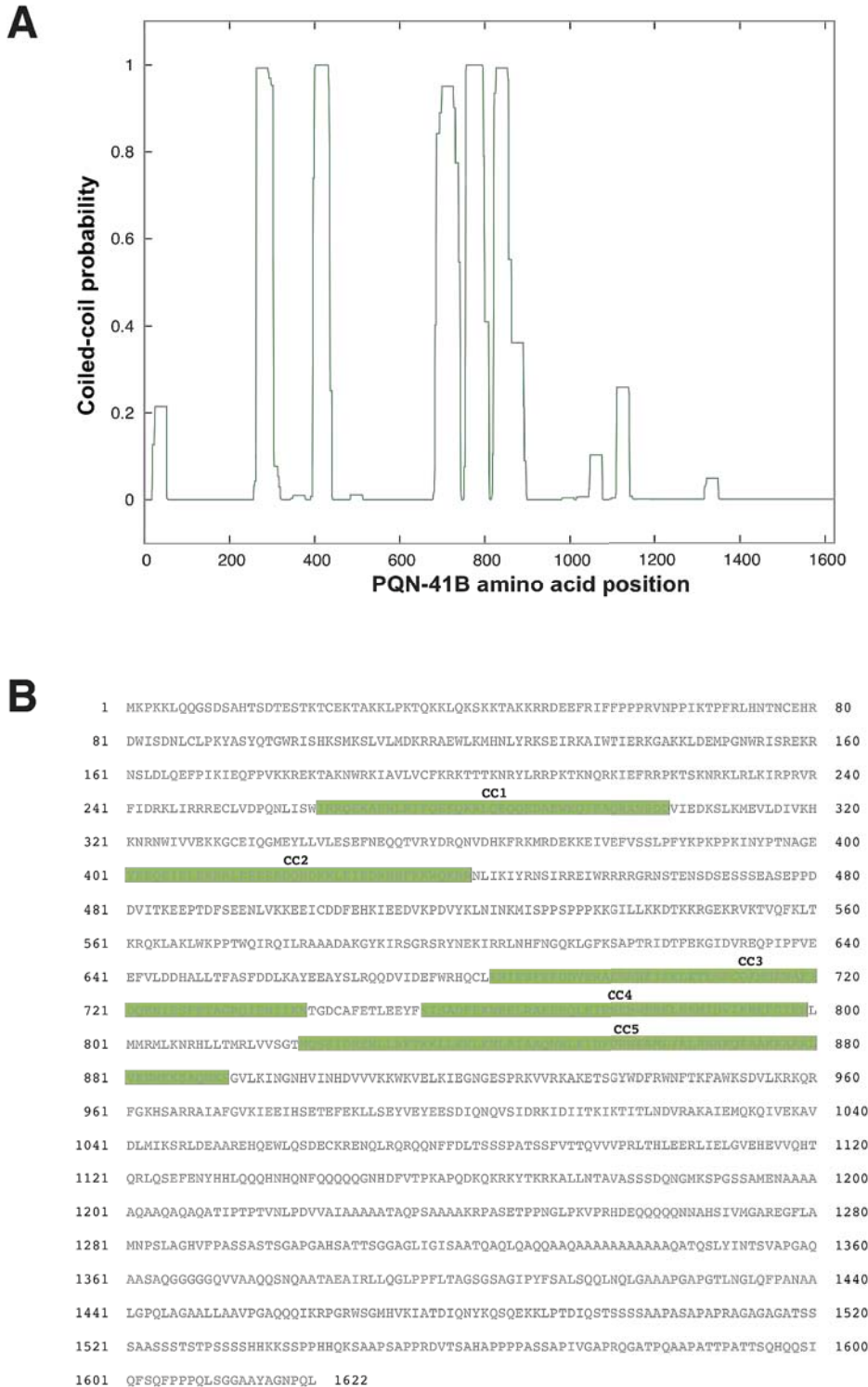


fig. S7. PQN-41B is also predicted to contain coiled-coil domains. **(A)** An analysis of coiled-coil formation probability of PQN-41B N-terminal sequences using the COILS algorithm (60), and a sliding window of 28 amino acids. **(B)** Annotation of predicted coiled-coil domains (Green) in the PQN-41B N-terminal protein sequence.

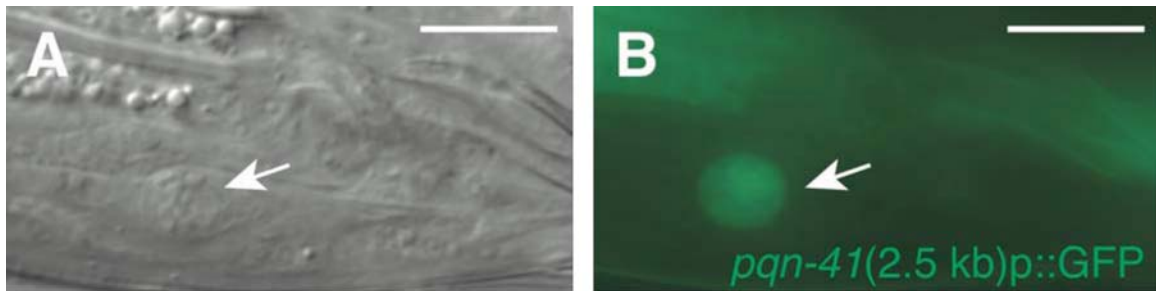


fig. S8. A 2.5 kb *pqn-41::GFP* reporter is expressed nearly exclusively in the linker cell as the cell begins to die. **(A)** Same as Fig. 3A except using the 2.5 kb *pqn-41::GFP* reporter in Fig. 2A. **(B)** Same as (A) except fluorescence image only. Scale bars, 10 μ m.

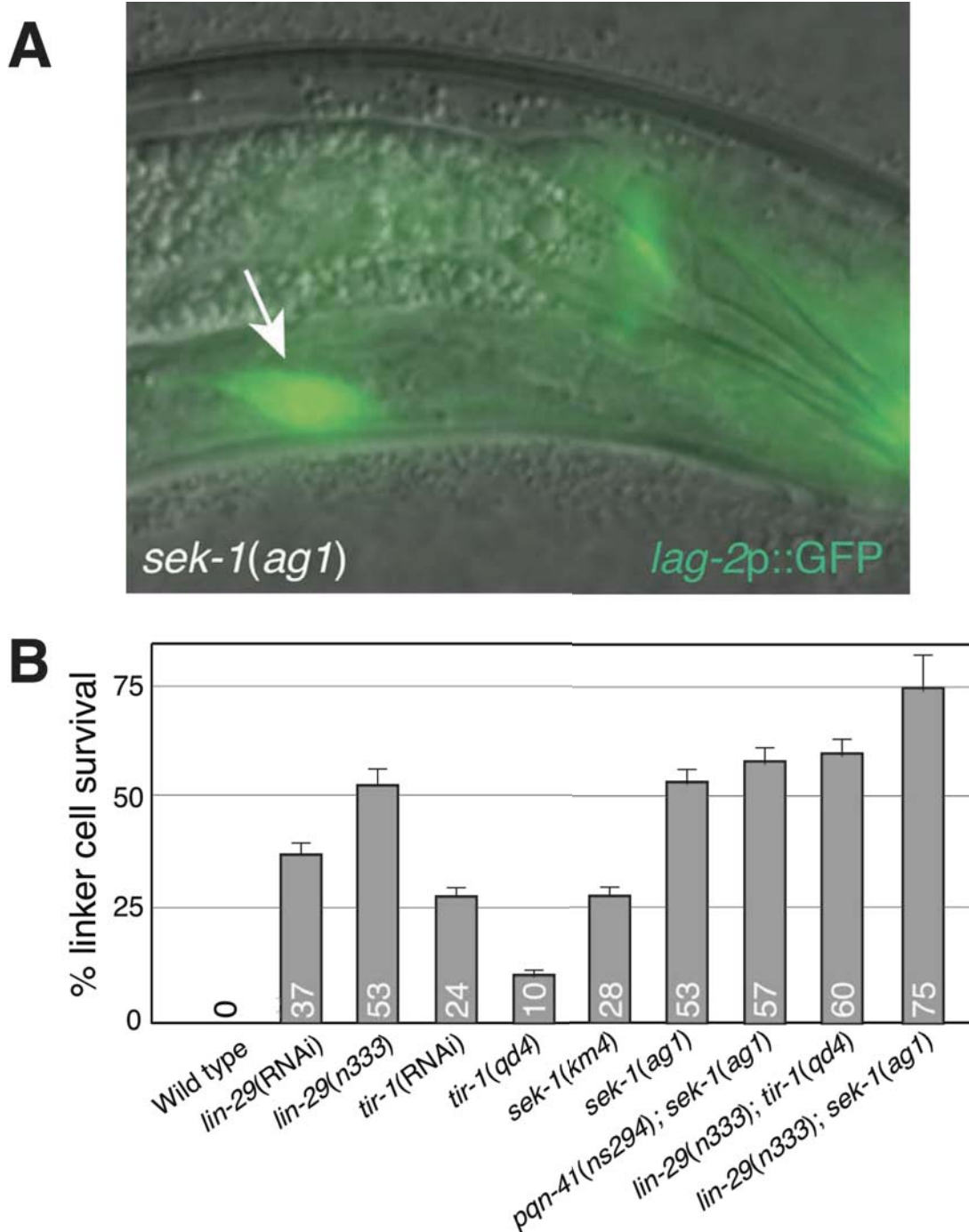


fig. S9. Mutations in *sek-1* block linker cell death. (A) Merged DIC and fluorescence image showing linker cell (arrow) survival in a young adult male of the indicated genotype. (B) Histogram depicting linker cell survival in the indicated strains. Number within bars, exact percentages. Error bars, SEM. $n \geq 87$ except for *lin-29*; *sek-1* where $n=28$.

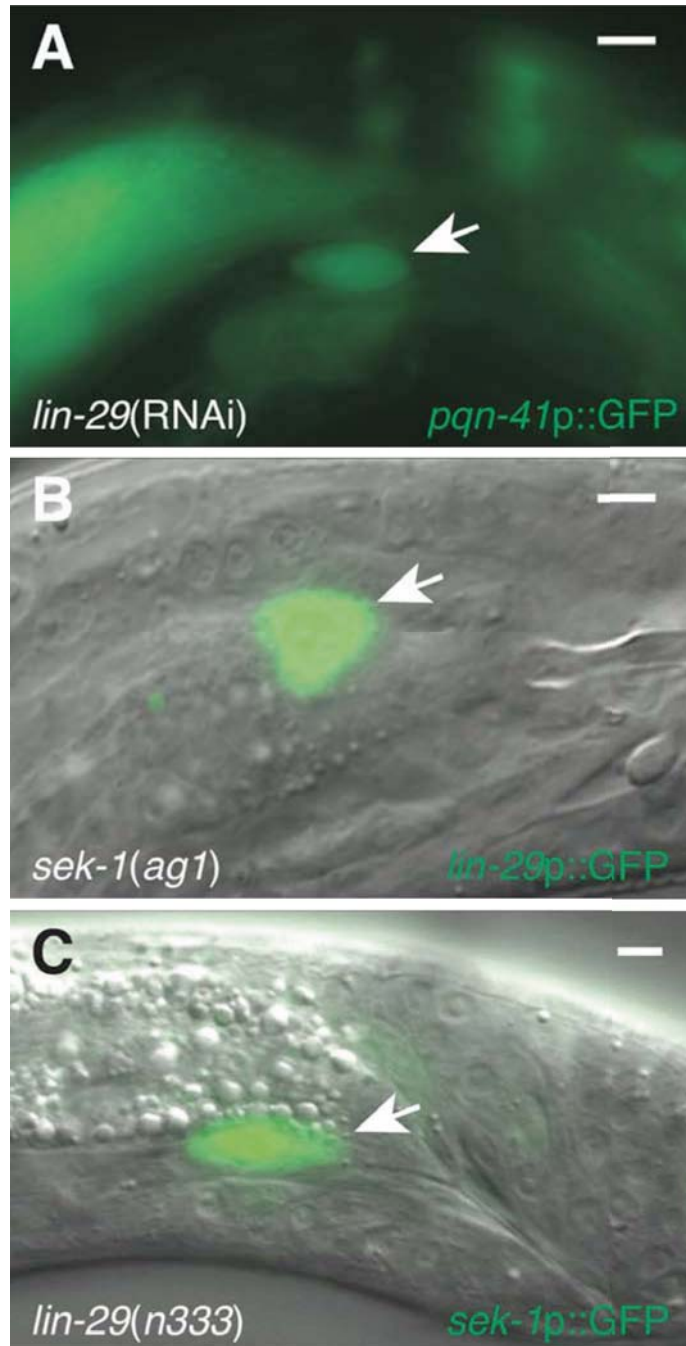


fig. S10. Transcription of *pqn-41*, *lin-29*, and *sek-1* in mutant backgrounds. (A) Fluorescence image of a young adult male with a surviving linker cell (arrow). The 2.5 kb *pqn-41::GFP* reporter was used. (B,C) Merged DIC and fluorescence image of young adult males of indicated genotypes and carrying indicated GFP transgenes. Scale bars, 5 μ m. Expression of *pqn-41* and *sek-1* GFP reporters in wild-type animals is shown in the main Figures 3 and 4; *lin-29* GFP reporter in wild-type was previously reported (8).

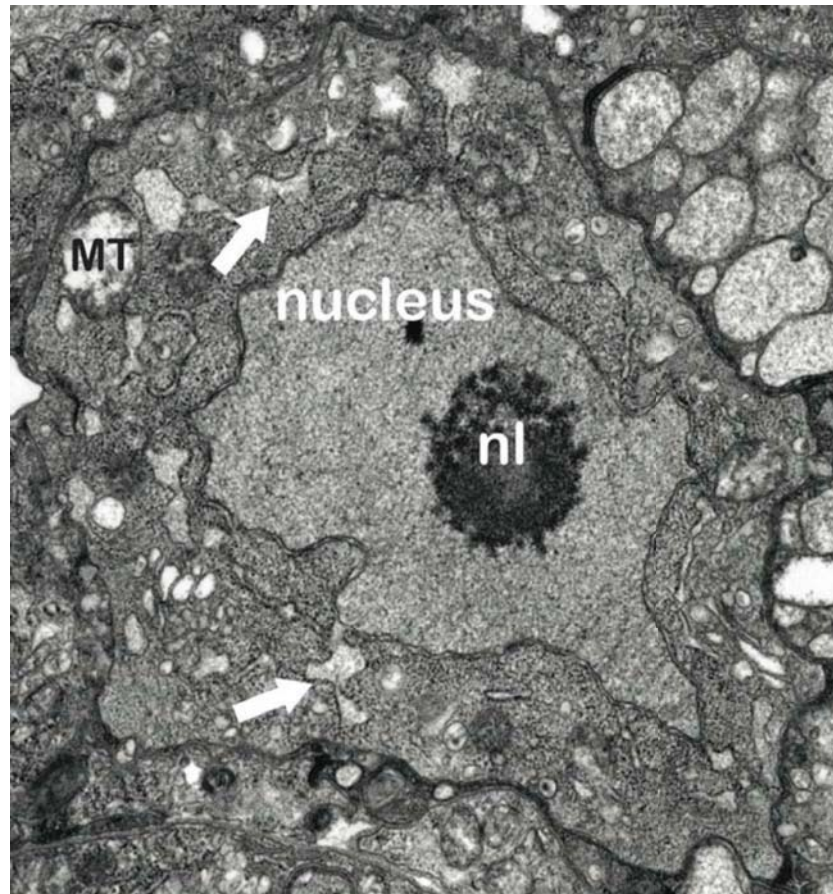


fig. S11. Electron micrograph of a surviving linker cell in a *lin-29(n333)* mutant. Although some swelling of the ER is evident (white arrows), the nuclear envelope remains generally intact and is not as severely dilated as in *pqn-41(ns294)* mutants. Note that mild crenellation of the nucleus is evident. MT, mitochondria. nl, nucleolus.

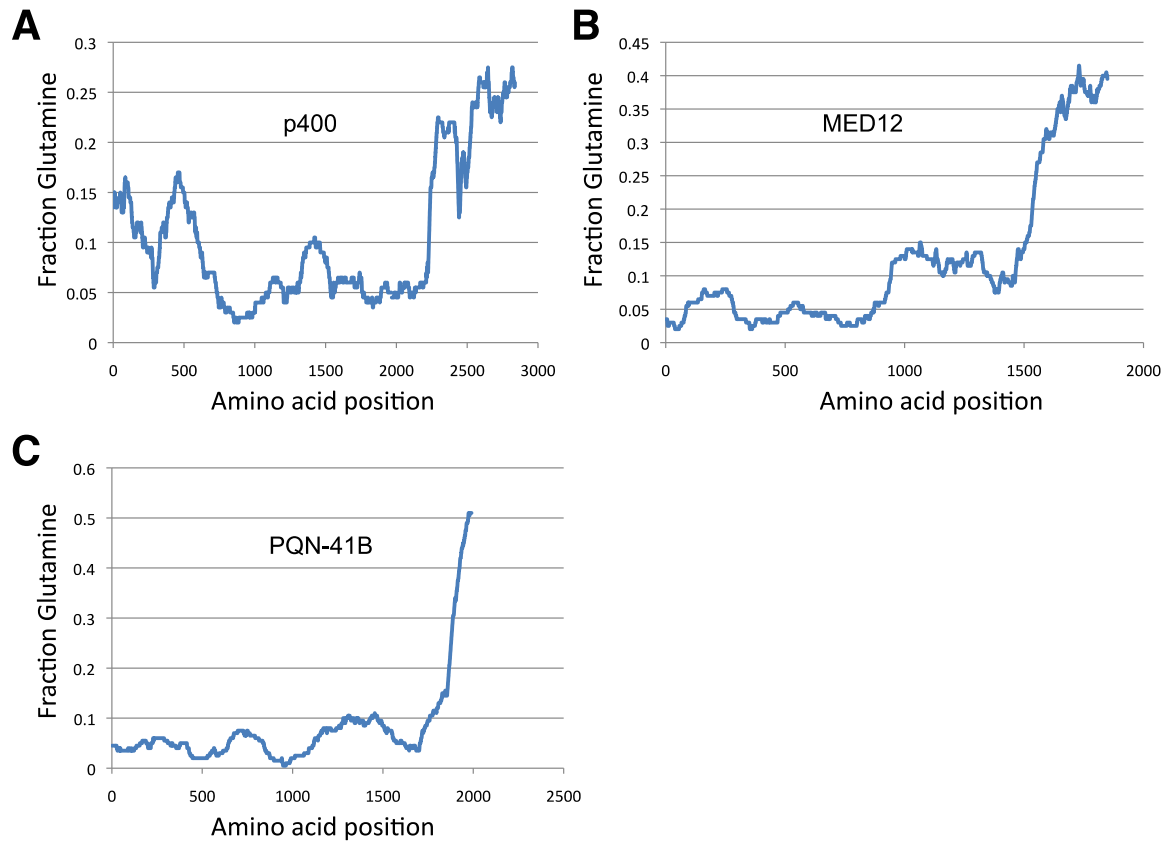


fig. S12. p400 and MED12 have polyglutamine tails. Graphs depict the fraction of amino acids that are glutamine in a 200 amino-acid sliding window initiating at the amino acid position indicated. (A) mouse p400. (B) mouse MED12. (C) *C. elegans* PQN-41B.

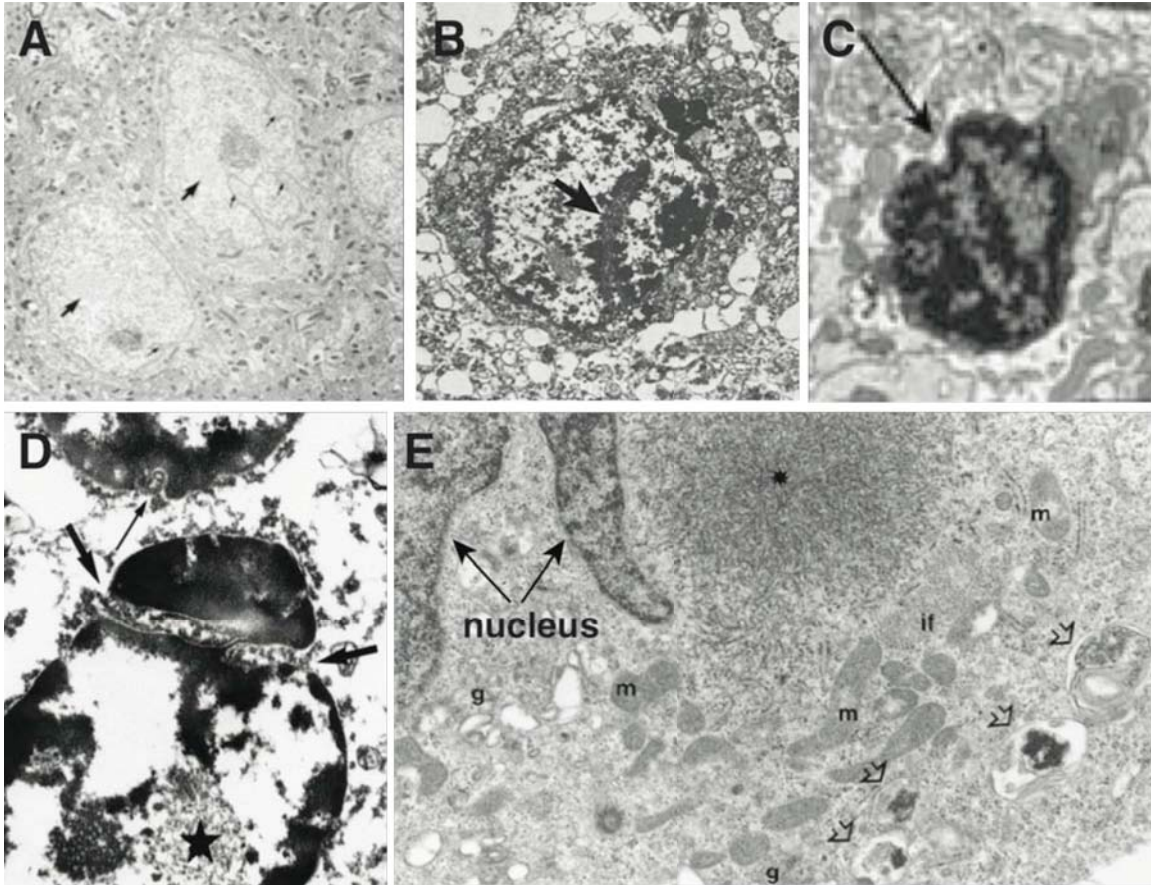


fig. S13. Electron micrographs of cells in patients, mouse, and cell culture models of polyQ disease demonstrating nuclear indentations. (A) Mouse model of Huntington's disease (HD) (61). Small arrows, nuclear indentations. (B) HD patient biopsy (62). Arrow, nuclear indentation. (C) Mouse model of SCA17 (63). Arrow, nuclear indentation. (D) DRPLA patient biopsy (64). Large arrows, nuclear indentation. (E) Cell culture model of SCA7 (65). Arrows, nuclear indentation. Images obtained by permission from the indicated references.

table S1. The unfolded protein response (UPR) is not required for linker cell death. Mutations in the indicated genes block the three known pathways leading to the UPR. All strains contain *qIs56*, an integrated GFP marker for the linker cell and *him-5(e1490)*. Linker cell survival was scored 2-4 hours after the L4-adult transition. In none of these strains was precocious linker cell death observed.

Genotype	% linker cell survival	n
<i>ire-1(v33)</i>	0	16
<i>xbp-1(zc12)</i>	0	64
<i>pek-1(ok275)</i>	4	104

table S2. p38 MAP kinase pathway kinases other than *sek-1* do not affect linker cell death. All strains contain *qIs56*, an integrated GFP marker for the linker cell and either *him-8(e1489)* or *him-5(e1490)*. The *mpk-1* allele was linked to the *unc-32(e189)* mutation. Linker cell survival was scored 2-4 hours after the L4-adult transition. n>86 for all strains.

Genotype	Process	% linker cell survival
<i>tol-1(nr2033)</i>	Innate immunity	1
p38 pathway kinases		
<i>nsy-1(ky397)</i>	Innate immunity, neuronal differentiation	1
<i>nsy-1(ky542)</i>	Innate immunity, neuronal differentiation	2
<i>sek-1(km4)</i>	Innate immunity, neuronal differentiation	20
<i>sek-1(ag1)</i>	Innate immunity, neuronal differentiation	49
<i>pmk-1(km25)</i>	Innate immunity	1
<i>pmk-3(ok169)</i>	Synaptic function, neuronal regeneration, stress response	6
Other MAPK pathway kinases		
<i>mpk-1(ku1)</i>	Ras signaling	0
<i>mtk-1(ok1382)</i>	Unknown	0
<i>jkk-1(km2)</i>	Synaptic function, stress response	2
<i>mek-1(ks54)</i>	Stress response	1
<i>mkk-4(ju91)</i>	Synaptic function	0
<i>jnk-1(gk7)</i>	Synaptic function, stress response	0
<i>kgb-1(km21)</i>	Stress response, neuronal regeneration	4
<i>kgb-2(gk361)</i>	Neuronal regeneration	2
<i>dlk-1(tm4024)</i>	Synaptic function, neuronal regeneration	2

References and Notes

1. M. C. Abraham, S. Shaham, Death without caspases, caspases without death. *Trends Cell Biol.* **14**, 184 (2004). [doi:10.1016/j.tcb.2004.03.002](https://doi.org/10.1016/j.tcb.2004.03.002) [Medline](#)
2. Y. Fuchs, H. Steller, Programmed cell death in animal development and disease. *Cell* **147**, 742 (2011). [doi:10.1016/j.cell.2011.10.033](https://doi.org/10.1016/j.cell.2011.10.033) [Medline](#)
3. J. F. Kerr, A. H. Wyllie, A. R. Currie, Apoptosis: A basic biological phenomenon with wide-ranging implications in tissue kinetics. *Br. J. Cancer* **26**, 239 (1972). [doi:10.1038/bjc.1972.33](https://doi.org/10.1038/bjc.1972.33) [Medline](#)
4. N. Honarpour *et al.*, Adult Apaf-1-deficient mice exhibit male infertility. *Dev. Biol.* **218**, 248 (2000). [doi:10.1006/dbio.1999.9585](https://doi.org/10.1006/dbio.1999.9585) [Medline](#)
5. E. Coucouvanis, G. R. Martin, Signals for death and survival: A two-step mechanism for cavitation in the vertebrate embryo. *Cell* **83**, 279 (1995). [doi:10.1016/0092-8674\(95\)90169-8](https://doi.org/10.1016/0092-8674(95)90169-8) [Medline](#)
6. W. Declercq, T. Vanden Berghe, P. Vandenabeele, RIP kinases at the crossroads of cell death and survival. *Cell* **138**, 229 (2009). [doi:10.1016/j.cell.2009.07.006](https://doi.org/10.1016/j.cell.2009.07.006) [Medline](#)
7. K. Newton, X. Sun, V. M. Dixit, Kinase RIP3 is dispensable for normal NF- κ Bs, signaling by the B-cell and T-cell receptors, tumor necrosis factor receptor 1, and Toll-like receptors 2 and 4. *Mol. Cell. Biol.* **24**, 1464 (2004). [doi:10.1128/MCB.24.4.1464-1469.2004](https://doi.org/10.1128/MCB.24.4.1464-1469.2004) [Medline](#)
8. M. C. Abraham, Y. Lu, S. Shaham, A morphologically conserved nonapoptotic program promotes linker cell death in *Caenorhabditis elegans*. *Dev. Cell* **12**, 73 (2007). [doi:10.1016/j.devcel.2006.11.012](https://doi.org/10.1016/j.devcel.2006.11.012) [Medline](#)
9. J. E. Sulston, D. G. Albertson, J. N. Thomson, The *Caenorhabditis elegans* male: postembryonic development of nongonadal structures. *Dev. Biol.* **78**, 542 (1980). [doi:10.1016/0012-1606\(80\)90352-8](https://doi.org/10.1016/0012-1606(80)90352-8) [Medline](#)
10. H. M. Ellis, H. R. Horvitz, Genetic control of programmed cell death in the nematode *C. elegans*. *Cell* **44**, 817 (1986). [doi:10.1016/0092-8674\(86\)90004-8](https://doi.org/10.1016/0092-8674(86)90004-8) [Medline](#)
11. G. Pilar, L. Landmesser, Ultrastructural differences during embryonic cell death in normal and peripherally deprived ciliary ganglia. *J. Cell Biol.* **68**, 339 (1976). [doi:10.1083/jcb.68.2.339](https://doi.org/10.1083/jcb.68.2.339) [Medline](#)
12. R. W. Oppenheim *et al.*, Programmed cell death of developing mammalian neurons after genetic deletion of caspases. *J. Neurosci.* **21**, 4752 (2001). [Medline](#)
13. T. Borsello, V. Mottier, V. Castagné, P. G. Clarke, Ultrastructure of retinal ganglion cell death after axotomy in chick embryos. *J. Comp. Neurol.* **453**, 361 (2002). [doi:10.1002/cne.10411](https://doi.org/10.1002/cne.10411) [Medline](#)
14. F. Simmer *et al.*, Loss of the putative RNA-directed RNA polymerase RRF-3 makes *C. elegans* hypersensitive to RNAi. *Curr. Biol.* **12**, 1317 (2002). [doi:10.1016/S0960-9822\(02\)01041-2](https://doi.org/10.1016/S0960-9822(02)01041-2) [Medline](#)
15. R. E. Ellis, H. R. Horvitz, Two *C. elegans* genes control the programmed deaths of specific cells in the pharynx. *Development* **112**, 591 (1991). [Medline](#)

16. H. Tabara *et al.*, The *rde-1* gene, RNA interference, and transposon silencing in *C. elegans*. *Cell* **99**, 123 (1999). [doi:10.1016/S0092-8674\(00\)81644-X](https://doi.org/10.1016/S0092-8674(00)81644-X) [Medline](#)
17. K. K. Tamai, K. Nishiwaki, bHLH transcription factors regulate organ morphogenesis via activation of an ADAMTS protease in *C. elegans*. *Dev. Biol.* **308**, 562 (2007). [doi:10.1016/j.ydbio.2007.05.024](https://doi.org/10.1016/j.ydbio.2007.05.024) [Medline](#)
18. F. Fiumara, L. Fioriti, E. R. Kandel, W. A. Hendrickson, Essential role of coiled coils for aggregation and activity of Q/N-rich prions and PolyQ proteins. *Cell* **143**, 1121 (2010). [doi:10.1016/j.cell.2010.11.042](https://doi.org/10.1016/j.cell.2010.11.042) [Medline](#)
19. P. W. Faber, C. Voisine, D. C. King, E. A. Bates, A. C. Hart, Glutamine/proline-rich PQE-1 proteins protect *Caenorhabditis elegans* neurons from huntingtin polyglutamine neurotoxicity. *Proc. Natl. Acad. Sci. U.S.A.* **99**, 17131 (2002). [doi:10.1073/pnas.262544899](https://doi.org/10.1073/pnas.262544899) [Medline](#)
20. N. T. Liberati *et al.*, Requirement for a conserved Toll/interleukin-1 resistance domain protein in the *Caenorhabditis elegans* immune response. *Proc. Natl. Acad. Sci. U.S.A.* **101**, 6593 (2004). [doi:10.1073/pnas.0308625101](https://doi.org/10.1073/pnas.0308625101) [Medline](#)
21. C. F. Chuang, C. I. Bargmann, A Toll-interleukin 1 repeat protein at the synapse specifies asymmetric odorant receptor expression via ASK1 MAPKKK signaling. *Genes Dev.* **19**, 270 (2005). [doi:10.1101/gad.1276505](https://doi.org/10.1101/gad.1276505) [Medline](#)
22. A. D. Johnson, D. Fitzsimmons, J. Hagman, H. M. Chamberlin, EGL-38 Pax regulates the ovo-related gene *lin-48* during *Caenorhabditis elegans* organ development. *Development* **128**, 2857 (2001). [Medline](#)
23. M. Fuchs *et al.*, The p400 complex is an essential E1A transformation target. *Cell* **106**, 297 (2001). [doi:10.1016/S0092-8674\(01\)00450-0](https://doi.org/10.1016/S0092-8674(01)00450-0) [Medline](#)
24. N. Mäkinen *et al.*, MED12, the mediator complex subunit 12 gene, is mutated at high frequency in uterine leiomyomas. *Science* **334**, 252 (2011). [doi:10.1126/science.1208930](https://doi.org/10.1126/science.1208930) [Medline](#)
25. S. Brenner, The genetics of *Caenorhabditis elegans*. *Genetics* **77**, 71 (1974). [Medline](#)
26. T. Stiernagle, in *WormBook*, The *C. elegans* Research Community, Ed.; available at <http://wormbook.org> (2006), pp. 1–11.
27. K. R. Siegfried, J. Kimble, POP-1 controls axis formation during early gonadogenesis in *C. elegans*. *Development* **129**, 443 (2002). [Medline](#)
28. J. Hodgkin, H. R. Horvitz, S. Brenner, Nondisjunction mutants of the nematode *Caenorhabditis elegans*. *Genetics* **91**, 67 (1979). [Medline](#)
29. J. L. Tenor, A. Aballay, A conserved Toll-like receptor is required for *Caenorhabditis elegans* innate immunity. *EMBO Rep.* **9**, 103 (2008). [doi:10.1038/sj.embor.7401104](https://doi.org/10.1038/sj.embor.7401104) [Medline](#)
30. V. Ambros, H. R. Horvitz, Heterochronic mutants of the nematode *Caenorhabditis elegans*. *Science* **226**, 409 (1984). [doi:10.1126/science.6494891](https://doi.org/10.1126/science.6494891) [Medline](#)

31. A. Sagasti *et al.*, The CaMKII UNC-43 activates the MAPKKK NSY-1 to execute a lateral signaling decision required for asymmetric olfactory neuron fates. *Cell* **105**, 221 (2001). [doi:10.1016/S0092-8674\(01\)00313-0](https://doi.org/10.1016/S0092-8674(01)00313-0) [Medline](#)
32. R. P. Shivers, T. Kooistra, S. W. Chu, D. J. Pagano, D. H. Kim, Tissue-specific activities of an immune signaling module regulate physiological responses to pathogenic and nutritional bacteria in *C. elegans*. *Cell Host Microbe* **6**, 321 (2009). [doi:10.1016/j.chom.2009.09.001](https://doi.org/10.1016/j.chom.2009.09.001) [Medline](#)
33. Y. Wu, M. Han, Suppression of activated Let-60 ras protein defines a role of *Caenorhabditis elegans* Sur-1 MAP kinase in vulval differentiation. *Genes Dev.* **8**, 147 (1994). [doi:10.1101/gad.8.2.147](https://doi.org/10.1101/gad.8.2.147) [Medline](#)
34. T. Mizuno *et al.*, The *Caenorhabditis elegans* MAPK phosphatase VHP-1 mediates a novel JNK-like signaling pathway in stress response. *EMBO J.* **23**, 2226 (2004). [doi:10.1038/sj.emboj.7600226](https://doi.org/10.1038/sj.emboj.7600226) [Medline](#)
35. K. Berman, J. McKay, L. Avery, M. Cobb, Isolation and characterization of pmk-(1-3): three p38 homologs in *Caenorhabditis elegans*. *Mol. Cell Biol. Res. Commun.* **4**, 337 (2001). [doi:10.1006/mcbr.2001.0300](https://doi.org/10.1006/mcbr.2001.0300) [Medline](#)
36. K. Nakata *et al.*, Regulation of a DLK-1 and p38 MAP kinase pathway by the ubiquitin ligase RPM-1 is required for presynaptic development. *Cell* **120**, 407 (2005). [doi:10.1016/j.cell.2004.12.017](https://doi.org/10.1016/j.cell.2004.12.017) [Medline](#)
37. A. Villanueva *et al.*, jkk-1 and mek-1 regulate body movement coordination and response to heavy metals through jnk-1 in *Caenorhabditis elegans*. *EMBO J.* **20**, 5114 (2001). [doi:10.1093/emboj/20.18.5114](https://doi.org/10.1093/emboj/20.18.5114) [Medline](#)
38. D. H. Kim *et al.*, A conserved p38 MAP kinase pathway in *Caenorhabditis elegans* innate immunity. *Science* **297**, 623 (2002). [doi:10.1126/science.1073759](https://doi.org/10.1126/science.1073759) [Medline](#)
39. M. Tanaka-Hino *et al.*, SEK-1 MAPKK mediates Ca²⁺ signaling to determine neuronal asymmetric development in *Caenorhabditis elegans*. *EMBO Rep.* **3**, 56 (2002). [doi:10.1093/embo-reports/kvf001](https://doi.org/10.1093/embo-reports/kvf001) [Medline](#)
40. M. Kawasaki *et al.*, A *Caenorhabditis elegans* JNK signal transduction pathway regulates coordinated movement via type-D GABAergic motor neurons. *EMBO J.* **18**, 3604 (1999). [doi:10.1093/emboj/18.13.3604](https://doi.org/10.1093/emboj/18.13.3604) [Medline](#)
41. M. Koga, R. Zwaal, K. L. Guan, L. Avery, Y. Ohshima, A *Caenorhabditis elegans* MAP kinase kinase, MEK-1, is involved in stress responses. *EMBO J.* **19**, 5148 (2000). [doi:10.1093/emboj/19.19.5148](https://doi.org/10.1093/emboj/19.19.5148) [Medline](#)
42. J. Ahringer, *WormBook* in *WormBook*, The *C. elegans* Research Community, Ed.; available at <http://wormbook.org> (2006).
43. R. S. Kamath, J. Ahringer, Genome-wide RNAi screening in *Caenorhabditis elegans*. *Methods* **30**, 313 (2003). [doi:10.1016/S1046-2023\(03\)00050-1](https://doi.org/10.1016/S1046-2023(03)00050-1) [Medline](#)
44. R. S. Kamath, M. Martinez-Campos, P. Zipperlen, A. G. Fraser, J. Ahringer, *Genome Biol.* **2**, RESEARCH0002 (2001).

45. A. G. Fraser *et al.*, Functional genomic analysis of *C. elegans* chromosome I by systematic RNA interference. *Nature* **408**, 325 (2000). [doi:10.1038/35042517](https://doi.org/10.1038/35042517) [Medline](#)
46. R. S. Kamath *et al.*, Systematic functional analysis of the *Caenorhabditis elegans* genome using RNAi. *Nature* **421**, 231 (2003). [doi:10.1038/nature01278](https://doi.org/10.1038/nature01278) [Medline](#)
47. J. F. Rual *et al.*, Toward improving *Caenorhabditis elegans* phenome mapping with an ORFeome-based RNAi library. *Genome Res.* **14**, (10B), 2162 (2004). [doi:10.1101/gr.2505604](https://doi.org/10.1101/gr.2505604) [Medline](#)
48. H. A. Hess, J. C. Röper, S. W. Grill, M. R. Koelle, RGS-7 completes a receptor-independent heterotrimeric G protein cycle to asymmetrically regulate mitotic spindle positioning in *C. elegans*. *Cell* **119**, 209 (2004). [doi:10.1016/j.cell.2004.09.025](https://doi.org/10.1016/j.cell.2004.09.025) [Medline](#)
49. G. Jansen, E. Hazendonk, K. L. Thijssen, R. H. Plasterk, Reverse genetics by chemical mutagenesis in *Caenorhabditis elegans*. *Nat. Genet.* **17**, 119 (1997). [doi:10.1038/ng0997-119](https://doi.org/10.1038/ng0997-119) [Medline](#)
50. C. C. Mello, J. M. Kramer, D. Stinchcomb, V. Ambros, Efficient gene transfer in *C. elegans*: extrachromosomal maintenance and integration of transforming sequences. *EMBO J.* **10**, 3959 (1991). [Medline](#)
51. M. Kato, P. W. Sternberg, The *C. elegans* tailless/Tlx homolog nhr-67 regulates a stage-specific program of linker cell migration in male gonadogenesis. *Development* **136**, 3907 (2009). [doi:10.1242/dev.035477](https://doi.org/10.1242/dev.035477) [Medline](#)
52. M. Maduro, D. Pilgrim, Identification and cloning of unc-119, a gene expressed in the *Caenorhabditis elegans* nervous system. *Genetics* **141**, 977 (1995). [Medline](#)
53. K. Roayaie, J. G. Crump, A. Sagasti, C. I. Bargmann, The G alpha protein ODR-3 mediates olfactory and nociceptive function and controls cilium morphogenesis in *C. elegans* olfactory neurons. *Neuron* **20**, 55 (1998). [doi:10.1016/S0896-6273\(00\)80434-1](https://doi.org/10.1016/S0896-6273(00)80434-1) [Medline](#)
54. M. A. Allen, L. W. Hillier, R. H. Waterston, T. Blumenthal, A global analysis of *C. elegans* trans-splicing. *Genome Res.* **21**, 255 (2011). [doi:10.1101/gr.113811.110](https://doi.org/10.1101/gr.113811.110) [Medline](#)
55. M. B. Gerstein *et al.*; modENCODE Consortium, Integrative analysis of the *Caenorhabditis elegans* genome by the modENCODE project. *Science* **330**, 1775 (2010). [doi:10.1126/science.1196914](https://doi.org/10.1126/science.1196914) [Medline](#)
56. M. Kirouac, P. W. Sternberg, cis-Regulatory control of three cell fate-specific genes in vulval organogenesis of *Caenorhabditis elegans* and *C. briggsae*. *Dev. Biol.* **257**, 85 (2003). [doi:10.1016/S0012-1606\(03\)00032-0](https://doi.org/10.1016/S0012-1606(03)00032-0) [Medline](#)
57. H. T. Schwartz, A protocol describing pharynx counts and a review of other assays of apoptotic cell death in the nematode worm *Caenorhabditis elegans*. *Nat. Protoc.* **2**, 705 (2007). [doi:10.1038/nprot.2007.93](https://doi.org/10.1038/nprot.2007.93) [Medline](#)
58. E. A. Lundquist, P. W. Reddien, E. Hartweg, H. R. Horvitz, C. I. Bargmann, Three *C. elegans* Rac proteins and several alternative Rac regulators control axon guidance, cell migration and apoptotic cell phagocytosis. *Development* **128**, 4475 (2001). [Medline](#)
59. J. Hodgkin, Exploring the envelope. Systematic alteration in the sex-determination system of the nematode *Caenorhabditis elegans*. *Genetics* **162**, 767 (2002). [Medline](#)

60. A. Lupas, M. Van Dyke, J. Stock, Predicting coiled coils from protein sequences. *Science* **252**, 1162 (1991). [doi:10.1126/science.252.5009.1162](https://doi.org/10.1126/science.252.5009.1162)
61. S. W. Davies *et al.*, Formation of neuronal intranuclear inclusions underlies the neurological dysfunction in mice transgenic for the HD mutation. *Cell* **90**, 537 (1997). [doi:10.1016/S0092-8674\(00\)80513-9](https://doi.org/10.1016/S0092-8674(00)80513-9) [Medline](#)
62. G. T. Bots, G. W. Bruyn, Neuropathological changes of the nucleus accumbens in Huntington's chorea. *Acta Neuropathol.* **55**, 21 (1981). [doi:10.1007/BF00691525](https://doi.org/10.1007/BF00691525) [Medline](#)
63. M. J. Friedman *et al.*, Polyglutamine domain modulates the TBP-TFIIB interaction: Implications for its normal function and neurodegeneration. *Nat. Neurosci.* **10**, 1519 (2007). [doi:10.1038/nn2011](https://doi.org/10.1038/nn2011) [Medline](#)
64. H. Takahashi *et al.*, Neuronal nuclear alterations in dentatorubral-pallidoluysian atrophy: Ultrastructural and morphometric studies of the cerebellar granule cells. *Brain Res.* **919**, 12 (2001). [doi:10.1016/S0006-8993\(01\)02986-9](https://doi.org/10.1016/S0006-8993(01)02986-9) [Medline](#)
65. C. Zander *et al.*, Similarities between spinocerebellar ataxia type 7 (SCA7) cell models and human brain: Proteins recruited in inclusions and activation of caspase-3. *Hum. Mol. Genet.* **10**, 2569 (2001). [doi:10.1093/hmg/10.22.2569](https://doi.org/10.1093/hmg/10.22.2569) [Medline](#)